Proceedings of the Sixteenth International Conference on
Computational Structures Technology
Edited by: P. Iványi, J. Kruis and B.H.V. Topping
Civil-Comp Conferences, Volume 14, Paper 10.2
Civil-Comp Press, Edinburgh, United Kingdom, 2026
ISSN: 2753-3239, doi: 10.4203/ccc.14.10.2


# A Hierarchical Hermite Finite Cell Framework for Strain Gradient Kirchhoff Plate Theory

**C. A. Yan[1], N. Fantuzzi[1], R. Vescovini[2] and R. Luciano[3]**

**[1] Università di Bologna, Italy**
**[2] Politecnico di Milano, Italy**
**[3] Università degli Studi di Napoli Parthenope, Italy**

## Abstract

Strain gradient plate theories are governed by partial differential equations of higher order than those in classical plate models, requiring higher continuous approximations. In the finite element method, the simplest way to satisfy these continuity requirements is to use Hermite interpolation polynomials. However, the construction of geometry-conforming Hermite elements significantly complicates mesh generation, particularly in complex domains.

In this work, the finite cell method is proposed to overcome these difficulties by decoupling the geometry representation from the field approximation. The physical domain is described on a nonconforming integration mesh, while the unknown field variables are approximated on a separate interpolation mesh defined over a simple background domain. To satisfy the continuity requirements inherent to strain gradient theories, a novel hierarchical Hermite polynomial space is introduced. Compared with the classical Hermite elements, the proposed formulation enables p-refinement of the numerical solution, leading to improved refinement flexibility.

The methodology is implemented within a Kirchhoff strain gradient plate theory and validated through free vibration problems involving complex geometries. Numerical results demonstrate high convergence of the solution, together with enhanced modeling flexibility enable by the finite cell method.

**Keywords:** strain gradient theory, Kirchhoff nanoplates, finite element method, hierarchical hermite functions, finite cell method, fictitious domain, complex geometries

# 1 Introduction

Strain gradient theories have gained increasing popularity in the modeling of thin nanostructures, as they provide an efficient mean to enrich the classical continuum theory without resorting to molecular dynamics simulations [1]. However, the use of strain gradient formulations has important implications for the development of numerical solution strategies. Due to the higher-order governing equations, these models require stricter smoothness requirements on the displacement field. In the specific case of the strain gradient Kirchhoff plate theory, this results in a $C^2$-continuity requirement across element boundaries. Within the framework of finite element methods, such continuity is commonly achieved through Hermite interpolation polynomials.

Several Hermite finite element formulations have been proposed in the literature. Classical examples include the $C^1$-conforming Bogner-Fox-Schmit (BFS) [2] and $C^1$-nonconforming Adini-Clough-Melosh (ACM) [3] elements. For $C^2$-continuous formulations, notable contributions are the conforming and nonconforming bending elements introduced by Babu and Patel [4], and the subsequent extensions by Bacciocchi et al. [5], who coupled these $C^2$-continuous bending elements with $C^1$-continuous membrane elements based on the BFS and ACM formulations.

While Hermite plate elements are straightforward to formulate, their practical implementation becomes challenging for complex geometries. The main difficulty lies in the isoparametric mapping between computational and physical element, originally developed for $C^0$-continuous formulations. For $C^1$-continuous Hermite elements, second-order derivatives must be consistently transformed under this mapping, which requires special treatment of the standard isoparametric procedure [6–10]. These difficulties become even more pronounced for $C^2$-continuous elements for which higher-order derivatives further complicates the implementation [11–13].

In this context, the finite cell method (FCM) [14] provides an attractive framework for simplifying the meshing procedure of complex geometries. By embedding the physical domain into a geometrically simple background domain, the FCM decouples geometric representation from solution approximation. The physical geometry is accounted for through numerical integration on a nonconforming mesh, whereas the solution field is represented on a structured background mesh of simple square elements for which the mapping is straightforward – even for Hermite-based discretizations.

A first attempt to combine the FCM with Hermite elements was presented in Ref.

[15], where a $C^1$-continuous Hermite discretization was employed to optimize the critical buckling load of Kirchhoff plates with complex cutouts. However, to the best of the authors' knowledge, this idea has not yet been extended to strain gradient Kirchhoff plate theory, which requires $C^2$-continuous approximations. Moreover, previous FCM-Hermite approaches rely on classical Hermite shape functions and are therefore restricted to $h$-refinement. This restricts the convergence potential of the FCM [16].

Motivated by these observations, this work aims to make two main contributions to the state-of-the-art. First, the FCM is extended for the first time to strain gradient Kirchhoff plate theory, eliminating the mapping complexities associated with $C^2$-continuous Hermite elements. Second, a novel hierarchical Hermite polynomial space is developed to fully leverage the convergence potential of the FCM. In contrast to classical Hermite formulations, the proposed approach preserves $C^2$-continuity while enabling systematic $p$-refinement.

The remainder of this paper is organized as follows: Section 2 briefly reviews the finite cell method. Its application to strain gradient Kirchhoff plate formulation is presented in Section 3. The hierarchical Hermite polynomial space employed for the finite element approximation is described in Section 4. Numerical results are discussed in Section 5, followed by concluding remarks in Section 6.

## 2 Finite cell method

The underlying idea of the finite cell method (FCM) is to solve the governing equations on an extended domain $\Omega$ that encloses the physical one $\Omega_{\text{phys}}$ [14]. The former is typically of rectangular shape, while the latter can have an arbitrarily complex geometry. This idea is illustrated in Figure 1 for a two-dimensional body with annular shape having boundary $\Gamma_{\text{phys}} = \Gamma_{\text{D}} \cup \Gamma_{\text{N}}$.

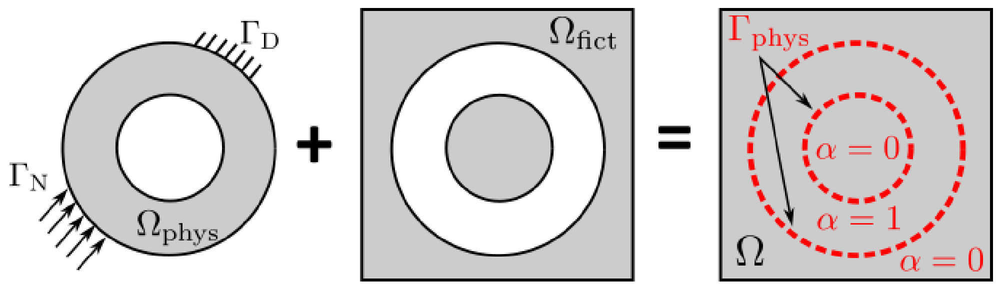


Figure 1: Main idea of the finite cell method.

The influence of the physical domain $\Gamma_{\text{phys}}$ is accounted for by a scalar function $\alpha$, which modifies the weak form of equilibrium as:

$$\int_{\Omega_{\text{phys}}} \mathcal{I}(\mathbf{x})\,\mathrm{d}\Omega_{\text{phys}} = \int_{\Omega} \alpha(\mathbf{x})\,\mathcal{I}(\mathbf{x})\,\mathrm{d}\Omega \quad \text{with} \quad \alpha(\mathbf{x}) = \begin{cases} 1, & \mathbf{x} \in \Omega_{\text{phys}} \\ 0, & \mathbf{x} \in \Omega_{\text{fict}} \end{cases}. \tag{1}$$

where $\mathbf{x} = \{x, y\}^{\mathrm{T}}$ is the vector of physical spatial coordinates, $\mathcal{I}(\mathbf{x})$ is the weak form integrand, while $\Omega_{\text{fict}} = \Omega \setminus \Omega_{\text{phys}}$ denotes the fictitious domain.

This formulation allows a simple, structured interpolation mesh to be used over $\Omega$, while the geometry complexity of the physical boundary $\Gamma_{\text{phys}}$ is accounted for via the integration procedure. In practice, a dedicated integration schemes, such as quadtree methods [17], are employed to accurately integrate elements cut by the physical boundary. An illustrative example is provided in Figure 2, where the geometry is captured by a nonconforming integration mesh with successive refinement levels $k$.

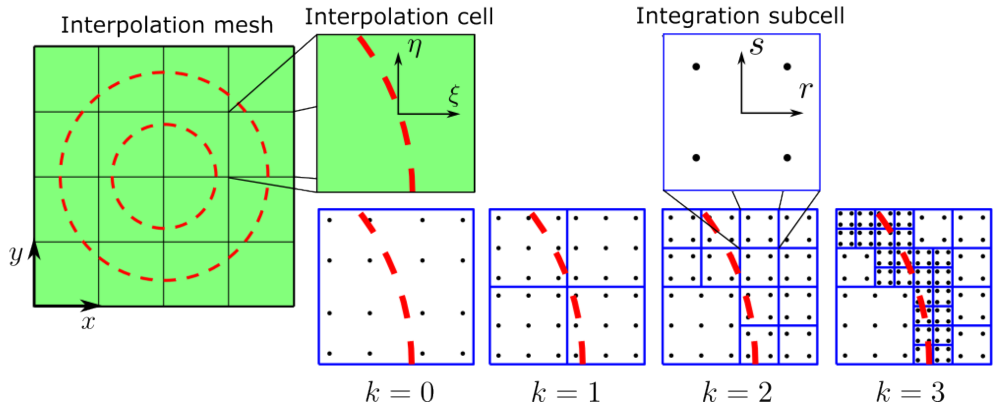


Figure 2: Quadtree integration scheme employed in the finite cell method.

Following this integration strategy, the weak form can then be approximated as:

$$\int_{\Omega} \alpha(\mathbf{x})\, \mathcal{I}(\mathbf{x})\, \mathrm{d}\Omega \simeq \sum_{i=1}^{N_{\mathrm{c}}} \int_{\Omega_i^{\mathrm{c}}} \alpha(\boldsymbol{\xi})\, \mathcal{I}(\boldsymbol{\xi}) \mathrm{d}\Omega_i^{\mathrm{c}} \simeq \sum_{i=1}^{N_{\mathrm{c}}} \sum_{j=1}^{N_{\mathrm{sc}}} \int_{\Omega_{ij}^{\mathrm{sc}}} \alpha(\mathbf{r})\, \mathcal{I}(\mathbf{r}) \mathrm{d}\Omega_{ij}^{\mathrm{sc}}, \tag{2}$$

where $N_{\mathrm{c}}$ is the number of interpolation elements, or sometimes called cells [14], and $N_{\mathrm{sc}}$ the number of integration subcells associated with each cell. The cell and subcell domains are denoted by $\Omega_i^{\mathrm{c}}$ and $\Omega_{ij}^{\mathrm{sc}}$ respectively, while $\boldsymbol{\xi} = \{\xi, \eta\}^{\mathrm{T}}$ and $\mathbf{r} = \{r, s\}^{\mathrm{T}}$ are the corresponding local coordinates.

Within the FCM, all the issues of meshing generation are avoided at the price of taking more sophisticated integration schemes, being the latter comparative easier than the former. In the following, this general framework is implemented within a Hermite-based strain gradient Kirchhoff finite element formulation, where the generation of suitable isoparametric mappings for meshing of complex geometries is particularly demanding.

# 3 Strain gradient Kirchhoff plate theory

This section briefly recalls the strain gradient Kirchhoff plate theory adopted in the present work. The constitutive relation of strain gradient elasticity are [18]:

$$\sigma_{ij} = C_{ijkl}(1 - l^2 \nabla^2)\epsilon_{kl}, \tag{3}$$

where $\sigma_{ij}$ and $\epsilon_{ij}$ are the stress and strain tensors, respectively, $C_{ijkl}$ is the fourth-order linear elastic stiffness tensor, $l$ is the material length-scale, while $\nabla^2 = \partial^2(\cdot)/\partial x^2 + \partial^2(\cdot)/\partial y^2$ represents the Laplacian operator.

In the framework of Kirchhoff plate theory, the in-plane strain components $\boldsymbol{\epsilon} = \{\epsilon_{xx}, \epsilon_{yy}, \gamma_{xy}\}^{\mathrm{T}}$ are expressed as:

$$\boldsymbol{\epsilon} = \boldsymbol{\epsilon}_{\mathrm{m}} + z\boldsymbol{\epsilon}_{\mathrm{b}} = \mathbb{D}_{\mathrm{m}}\mathbf{u} + z\mathbb{D}_{\mathrm{b}}\mathbf{u}, \tag{4}$$

where $\boldsymbol{\epsilon}_{\mathrm{m}}$ and $\boldsymbol{\epsilon}_{\mathrm{b}}$ are the generalized membrane strains and curvatures, whereas $\mathbf{u} = \{u, v, w\}^{\mathrm{T}}$ is the vector of mid-plane displacements. These latter are related to the three-dimensional displacement field $\mathbf{U} = \{u_x, u_y, u_z\}^{\mathrm{T}}$ through:

$$\mathbf{U} = (\mathbf{I} + z\mathbb{D}_{\mathrm{s}})\,\mathbf{u}, \tag{5}$$

where $\mathbf{I}$ is a $3 \times 3$ identity tensor, while the matrices of differential operator $\mathbb{D}$ are:

$$\mathbb{D}_{\mathrm{m}} = \begin{bmatrix} (\cdot)_{,x} & 0 & 0 \\ 0 & (\cdot)_{,y} & 0 \\ (\cdot)_{,y} & (\cdot)_{,x} & 0 \end{bmatrix}, \quad \mathbb{D}_{\mathrm{b}} = \begin{bmatrix} 0 & 0 & -(\cdot)_{,xx} \\ 0 & 0 & -(\cdot)_{,yy} \\ 0 & 0 & -2(\cdot)_{,xy} \end{bmatrix}, \quad \mathbb{D}_{\mathrm{s}} = \begin{bmatrix} 0 & 0 & (\cdot)_{,x} \\ 0 & 0 & (\cdot)_{,y} \\ 0 & 0 & 0 \end{bmatrix}, \tag{6}$$

with $(\cdot)_{,\beta} = \partial(\cdot)/\partial\beta$ denoting partial differentiation with respect to $\beta$.

The weak form integrand of the strain gradient Kirchhoff plate formulation is:

$$\begin{aligned} \mathcal{I}(\mathbf{x}) = {} & (\mathbb{D}_{\mathrm{m}}\delta\mathbf{u})^{\mathrm{T}} (\mathbf{A}\mathbb{D}_{\mathrm{m}} + \mathbf{B}\mathbb{D}_{\mathrm{b}})\,\mathbf{u} + (\mathbb{D}_{\mathrm{b}}\delta\mathbf{u})^{\mathrm{T}} (\mathbf{B}\mathbb{D}_{\mathrm{m}} + \mathbf{D}\mathbb{D}_{\mathrm{b}})\,\mathbf{u} + \\ & + l^2 \Big[ (\mathbb{D}_{\mathrm{m},x}\delta\mathbf{u})^{\mathrm{T}} (\mathbf{A}\mathbb{D}_{\mathrm{m},x} + \mathbf{B}\mathbb{D}_{\mathrm{b},x})\,\mathbf{u} + (\mathbb{D}_{\mathrm{b},x}\delta\mathbf{u})^{\mathrm{T}} (\mathbf{B}\mathbb{D}_{\mathrm{m},x} + \mathbf{D}\mathbb{D}_{\mathrm{b},x})\,\mathbf{u} + \\ & \quad + (\mathbb{D}_{\mathrm{m},y}\delta\mathbf{u})^{\mathrm{T}} (\mathbf{A}\mathbb{D}_{\mathrm{m},y} + \mathbf{B}\mathbb{D}_{\mathrm{b},y})\,\mathbf{u} + (\mathbb{D}_{\mathrm{b},y}\delta\mathbf{u})^{\mathrm{T}} (\mathbf{B}\mathbb{D}_{\mathrm{m},y} + \mathbf{D}\mathbb{D}_{\mathrm{b},y})\,\mathbf{u} \Big] + \\ & \quad + \delta\mathbf{u}^{\mathrm{T}}\mathbf{I}_0\ddot{\mathbf{u}} - \delta\mathbf{u}^{\mathrm{T}}\mathbf{I}_1 (\mathbb{D}_{\mathrm{s}}\ddot{\mathbf{u}}) - (\mathbb{D}_{\mathrm{s}}\delta\mathbf{u})^{\mathrm{T}}\mathbf{I}_1\ddot{\mathbf{u}} + (\mathbb{D}_{\mathrm{s}}\delta\mathbf{u})^{\mathrm{T}}\mathbf{I}_2 (\mathbb{D}_{\mathrm{s}}\ddot{\mathbf{u}}), \end{aligned} \tag{7}$$

where $\mathbf{A}$, $\mathbf{B}$, $\mathbf{D}$ are the membrane, membrane-bending coupling, bending stiffness matrices from classical lamination theory, respectively, while $\mathbf{I}_0$, $\mathbf{I}_1$, $\mathbf{I}_2$ are the $3 \times 3$ diagonal matrix collecting the mass moment of inertia of the plate ($I_0$, $I_1$, $I_2$).

Compared to classical elasticity for which $l = 0$, the strain gradient formulation introduces higher-order derivative terms, i.e. second-derivative terms of the membrane displacements and third-order terms of the transverse one. Consequently, $C^1$-continuity is required for the displacement components $u$ and $v$, while $C^2$-continuity for the component $w$. To satisfy these continuity requirements, a novel hierarchical Hermite function space is proposed in the following section.

# 4 Hierarchical Hermite polynomials

The proposed hierarchical Hermite polynomial space extends the classical Hermite interpolation by enabling systematic $p$-refinement in addition to standard $h$-refinement. This enables to fully exploits the high-order convergence properties of the FCM [16] while satisfying the continuity requirements of strain gradient Kirchhoff plate theory. In the following, two polynomial spaces are introduced to approximate the membrane and transverse displacement fields. These are denoted as the $C^1$-type and $C^2$-type hierarchical Hermite spaces, respectively.

## 4.1 $C^1$-type hierarchical Hermite

The $C^1$-type hierarchical Hermite functions are defined through the tensor product of the one-dimensional polynomials:

$$
\begin{aligned}
f_1(\xi) &= \frac{(1-\xi)^2(2+\xi)}{4}, & f_2(\xi) &= \frac{(1-\xi)^2(1+\xi)}{4},\\
f_3(\xi) &= \frac{(1+\xi)^2(2-\xi)}{4}, & f_4(\xi) &= \frac{(1+\xi)^2(\xi-1)}{4},\\
f_{i+1}(\xi) &= \sqrt{\frac{2i-1}{2}}\iint_{-1}^{\xi} P_{i-1}(\xi')\mathrm{d}\xi' & \text{for}\quad & i=4,5,...p.
\end{aligned}
\tag{8}
$$

Here, $p$ denotes the order of the polynomial space, $f_1 - f_4$ are cubic Hermite polynomial ensuring continuity of the displacement and its first derivative [2,3]. The higher-order functions $f_{i+1}$ are internal enrichment terms derived from the double integrals of Legendre polynomials $P_i$. These latter polynomials satisfy the properties:

$$
\begin{aligned}
& f_{i+1}(\pm 1) = \frac{\mathrm{d}f_{i+1}(\pm 1)}{\mathrm{d}\xi} = 0,\\
& \int_{-1}^{+1} \frac{\mathrm{d}^2 f_{i+1}}{\mathrm{d}\xi^2}\frac{\mathrm{d}^2 f_{j+1}}{\mathrm{d}\xi^2} = \begin{cases} 1 & \text{if} \quad i=j \\ 0 & \text{if} \quad i\neq j \end{cases} .
\end{aligned}
\tag{9}
$$

The first of Eq. (9) ensures that the internal functions do not interfere with the boundary degrees of freedom represented by $f_1 - f_4$, while the second of Eq. (9) states that their second derivatives are orthonormal.

## 4.2 $C^2$-type hierarchical Hermite

The $C^2$-type hierarchical Hermite functions are assembled using the tensor product of the following functions:

$$
\begin{aligned}
g_1(\xi) &= \frac{(1-\xi)^3\,(8+9\xi+3\xi^2)}{16}, & g_2(\xi) &= \frac{(1-\xi)^3(1+\xi)\,(5+3\xi)}{16},\\
g_3(\xi) &= \frac{(1-\xi)^3(1+\xi)^2}{16}, & g_4(\xi) &= \frac{(1+\xi)^3\,(8-9\xi+3\xi^2)}{16},\\
g_5(\xi) &= \frac{(1+\xi)^3(1-\xi)\,(5-3\xi)}{16}, & g_6(\xi) &= \frac{(1+\xi)^3(1-\xi)^2}{16}\\
g_{i+1}(\xi) &= \sqrt{\frac{2i-1}{2}}\iiint_{-1}^{\xi} P_{i-3}(\xi')\mathrm{d}\xi' & \text{for}\quad & i=6,5,...,p,
\end{aligned}
\tag{10}
$$

where $g_1 - g_6$ are quintic Hermite functions which enforce continuity of the displacement, as well as its first and second derivatives [4, 5]. The enrichment functions $g_{i+1}$ are obtained by triple integration of Legendre polynomials so to satisfy:

$$
\begin{aligned}
g_{i+1}(\pm 1) = \frac{\mathrm{d}g_{i+1}(\pm 1)}{\mathrm{d}\xi} = \frac{\mathrm{d}^2 g_{i+1}(\pm 1)}{\mathrm{d}\xi^2} = 0 \\
\int_{-1}^{+1} \frac{\mathrm{d}^3 g_{i+1}}{\mathrm{d}^3\xi} \frac{\mathrm{d}^3 g_{j+1}}{\mathrm{d}\xi^3} = \begin{cases} 1 & \text{if} \quad i = j \\ 0 & \text{if} \quad i \neq j \end{cases} \quad .
\end{aligned} \tag{11}
$$

These conditions ensure that the internal functions do not interfere with the boundary DOFs ($g_1 - g_6$) and their third derivatives are orthogonal.

The properties in Eqs. (9) and (11) are similar to those of the hierarchical bases first introduced by Babuška et. al [19] for $C^0$-continuous formulations, but here extended to satisfy the $C^1$- and $C^2$-continuity requirements. Similar to the $C^0$-continuous counterpart, these two spaces retain a hierarchical structure, exhibit improved conditioning of the stiffness matrix, and enable spectral convergence under $p$-refinement.

# 5 Results

To validate the proposed finite element formulation based on the finite cell method (FCM) and hierarchical Hermite polynomials, we consider the free vibration analysis of a square nanoplate with a heart-shaped cutout, originally proposed in Ref. [20].

The problem setup is illustrated in Figure 3a. The plate has side length $L = 5$ and thickness $t = 0.2$, with material properties $E = 10^7$, $\nu = 0.3$ and $\rho = 1000$. The nonlocal parameter is set to $l = 0.2$. Simply supported boundary conditions are applied along all edges. The interpolation mesh consists of $2 \times 2$ elements, as shown in Figure 3b, while the corresponding integration mesh is depicted in Figure 3c.

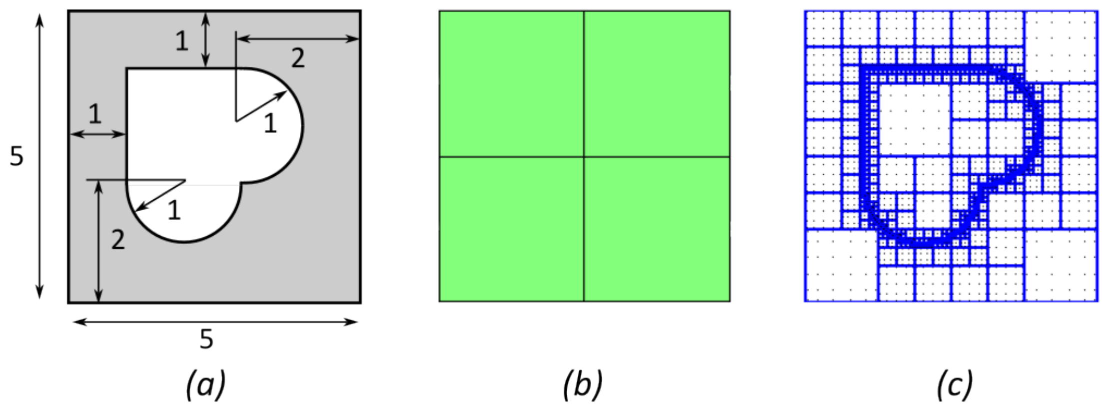


Figure 3: Heart-shaped Kirchhoff nanoplate problem: (a) geometry, (b) interpolation mesh, (c) integration mesh.

In the following, a two-step convergence analysis is performed. First, the resolution of the integration mesh is investigated. Second, with the converged integration scheme, the interpolation space is enriched through hierarchical $p$-refinement to assess the approximation performance of the proposed hierarchical Hermite elements.

## 5.1 Integration mesh convergence

The polynomial order of the interpolation space is initially fixed at $p = 5$, while successive refinements of the integration mesh are applied near the cutout. Figure 4 shows the convergence of the integration mesh resolution on the first four natural frequencies, $\omega_n$ ($n = 1, 2, 3, 4$). The results are normalized with respect to reference solutions ($\omega_n^{\text{ref}}$) obtained with a highly refined integration mesh ($k = 15$).

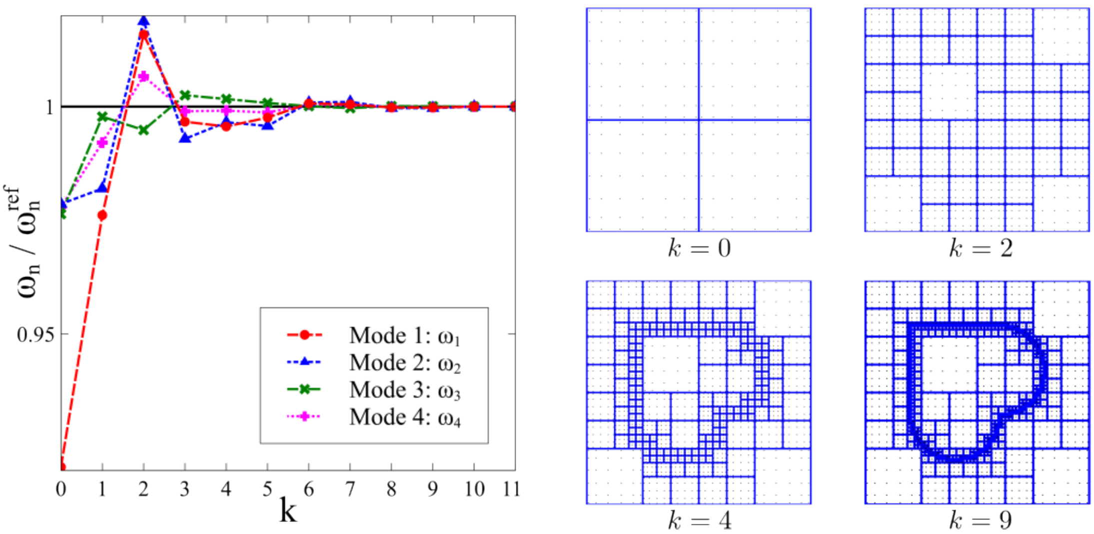


Figure 4: Convergence of the integration mesh.

For coarse integration meshes ($k < 6$), large oscillations are observed due to insufficient geometric resolution. These oscillations vanish beyond a refinement level of $k = 9$, indicating that the integration errors become negligible. This integration mesh is adopted in the subsequent analysis.

## 5.2 Interpolation mesh convergence

Using the converged integration mesh, the interpolation space is now enriched through hierarchical $p$-refinement. The polynomial order is increased from the minimum admissible $p = 5$ up to $p = 10$, without modifying the background mesh. The first four natural frequencies are reported in Table 1 together with the number of bending degrees of freedom (DOFs) for each interpolation order.

| | Refinement | DOFs | Mode 1 | Mode 2 | Mode 3 | Mode 4 |
|---|---|---|---|---|---|---|
| Hierarchical Hermite | $p = 5$ | 45 | 6.0541 | 11.8448 | 12.6938 | 19.7690 |
| | $p = 6$ | 69 | 6.0085 | 10.9615 | 12.1840 | 19.3598 |
| | $p = 7$ | 101 | 5.9846 | 10.6784 | 11.9972 | 19.2054 |
| | $h = 8$ | 141 | 5.9747 | 10.5520 | 11.8988 | 19.0877 |
| | $p = 9$ | 189 | 5.9720 | 10.5079 | 11.8494 | 19.0347 |
| | $p = 10$ | 245 | 5.9711 | 10.4934 | 11.8216 | 19.0137 |
| Wang et. al (2021) [21] | | | 5.99 | 10.54 | 11.76 | 19.11 |

Table 1: Convergence of natural frequencies upon interpolation space refinement.

The computed frequencies decrease monotonically with increasing $p$, indicating consistent convergence and confirming the adequacy of the chosen integration scheme. Rapid convergence performance is observed. With a polynomial order of $p = 9$, the results are accurate to approximately two significant digits, demonstrating the efficiency of the proposed formulation. Furthermore, comparison of the converged solutions with the ones reported by Wang et. al [21] shows excellent agreement with differences below $1\%$.

# 6 Concluding remarks

This work presented a finite element framework for strain gradient Kirchhoff plate theory that combines the finite cell method (FCM) with a novel hierarchical Hermite polynomial space. The proposed approach addresses a major challenge in strain gradient finite element formulations based on Hermite polynomials, i.e. the isoparametric mapping of distorted elements.

To address this issue, the physical domain is embedded into a simple, structured background mesh of square elements within the FCM. This strategy eliminates the need for distorted elements to conform to the physical boundary of the plate, leading to a much simpler mapping procedure.

A key limitation of existing Hermite polynomial spaces is that they typically allow only $h$-refinement of the numerical solution, thus restricting the convergence potential of the FCM. In this work, this restriction is removed by introducing a hierarchical enrichment of the classical Hermite basis to enable flexible $p$-refinement.

The framework was validated through the free vibration analysis of a cutout nanoplate. The study on the integration scheme demonstrated that accurate geometric representation can be achieved by adaptive refinement of the integration mesh. Moreover, the convergence study of the proposed hierarchical polynomial space showed monotonic and rapid error decrease.

In summary, the proposed formulation combines the simplicity of Hermite discretizations with the geometric flexibility of the FCM and the convergence performance of hierarchical $p$-refinement. This approach represents an efficient and versatile computational strategy for solving strain gradient plate problems.

## Acknowledgements

This work has been supported by the Ministry of University Research (MUR) PRIN 2020 project 2020F23HZ7_003 (CUP: J35F22000640001), PRIN 2022 project 2022YLNJRY (CUP: J53D23002500006) which is funded by the European Union - NextGenerationEU.


# References


[1] H. Askes, E.C. Aifantis, "Gradient elasticity in statics and dynamics: an overview of formulations, length scale identification procedures, finite element implementations and new results", International Journal of Solids and Structures, 48(13), 1962-1990, 2011.

[2] F.K. Bogner, R.L. Fox, L.A. Schmit, "The generation of inter-element-compatible stiffness and mass matrices by the use of interpolation formulae", In: Matrix Methods in Structural Mechanics Proceedings. Wright-Patterson Air Force Base, 397, 1965.

[3] R.J. Melosh, "Basis for derivation of matrices for the direct stiffness method", AIAA Journal, 1(7), 1631-1637, 1963.

[4] B. Babu, B.P. Patel, "A new computationally efficient finite element formulation for nanoplates using second-order strain gradient Kirchhoff's plate theory", Composites Part B: Engineering, 168, 302-311, 2019

[5] M. Bacciocchi, N. Fantuzzi, A.J.M. Ferreira, "Conforming and nonconforming laminated finite element Kirchhoff nanoplates in bending using strain gradient theory". Computers & Structures, 239, 106322, 2020.

[6] J. Petera, J.F.T. Pittman, "Isoparametric hermite elements", International Journal for Numerical Methods in Engineering, 37(20), 3489-3519, 1994.

[7] E.O. Frind, "An isoparametric Hermitian element for the solution of field problems", International Journal for Numerical Methods in Engineering, 11(6), 945-962, 1977.

[8] S. Virtanen, A. Pramila, "A refined Hermitian isoparametric plate bending element", Communications in Applied Numerical Methods, 4(1), 67-77, 1988.

[9] A. Beheshti, "Novel quadrilateral elements based on explicit Hermite polynomials for bending of Kirchhoff–Love plates", Computational Mechanics, 62(5), 1199-1211, 2018.

[10] L. Greco, M. Cuomo, L. Contrafatto, "A quadrilateral G1-conforming finite element for the Kirchhoff plate model", Computer Methods in Applied Mechanics and Engineering, 346, 913-951, 2019.

[11] B. Babu, B.P. Patel, "An improved quadrilateral finite element for nonlinear second-order strain gradient elastic Kirchhoff plates", Meccanica, 55(1), 139-159, 2020.

[12] M. Bacciocchi, N. Fantuzzi, "On the mapping procedure based on higher-order Hermite polynomials for laminated thin plates with arbitrary domains in gra-

dient elasticity", International Journal for Numerical Methods in Engineering, 124(11), 2552-2570, 2023.

[13] M. Bacciocchi, N. Fantuzzi, "Free vibrations and bending of laminated thin plates with distorted domains in gradient elasticity: an isoparametric finite element formulation based on Hermite mapping", Acta Mechanica, 1-21, 2025.

[14] J. Parvizian, A. Düster, E. Rank. "Finite cell method: h-and p-extension for embedded domain problems in solid mechanics", Computational Mechanics, 41(1), 121-133, 2007.

[15] S. Eisenträger, J. Kiendl, G. Michaloudis, R. Duy, Y. Vetyukov, "Stability analysis of plates using cut Bogner-Fox-Schmit elements", Computers & Structures, 270, 106854, 2022.

[16] M. Dauge, A. Düster, E. Rank, "Theoretical and numerical investigation of the finite cell method", Journal of Scientific Computing, 65(3), 1039-1064, 2015.

[17] A. Abedian, J. Parvizian, A. Düster, H. Khademyzadeh, E. Rank, "Performance of different integration schemes in facing discontinuities in the finite cell method", International Journal of Computational Methods, 10(03), 1350002, 2012.

[18] E.C. Aifantis, "On the role of gradients in the localization of deformation and fracture", International Journal of Engineering Science, 30(10), 1279-1299, 1992.

[19] I. Babuška, B.A. Szabó, I.N. Katz, "The p-version of the finite element method", SIAM Journal on Numerical Analysis, 18(3), 515-545, 1981.

[20] C.H. Thai, A.M. Zenkour, M.A. Wahab, H. Nguyen-Xuan, "A simple four-unknown shear and normal deformations theory for functionally graded isotropic and sandwich plates based on isogeometric analysis". Composite Structures, 139, 77-95, 2016.

[21] B. Wang, C. Lu, C. Fan, M. Zhao, "A meshfree method with gradient smoothing for free vibration and buckling analysis of a strain gradient thin plate", Engineering Analysis with Boundary Elements, 132, 159-167, 2021.